**Proceedings of the ASME 2018 International Mechanical Engineering Congress and Exposition**
**IMECE2018**
**November 9-15, 2018, Pittsburgh, PA, USA**

# IMECE2018-88172

# ATOMISTIC SIMULATIONS OF MECHANICAL PROPERTIES OF CIRCULAR AND COLLAPSED CARBON NANOTUBES WITH COVALENT CROSS-LINKS

**Arun B. Thapa**
abthapa@crimson.ua.edu
Department of Mechanical Engineering
University of Alabama
Tuscaloosa, Alabama, USA

**Alexey N. Volkov**
avolkov1@ua.edu
Department of Mechanical Engineering
University of Alabama
Tuscaloosa, Alabama, USA

## ABSTRACT

Stretching properties of single-walled carbon nanotubes (CNTs) of large diameters are studied in atomistic simulations. The simulations are performed based on the AIREBO empirical interatomic potential for three types of CNTs: Nanotubes with circular cross section, permanently collapsed nanotubes with "dog-bone"-shaped cross sections, and collapsed nanotubes with intra-tube covalent cross-links. In the last case, the cross-links between parallel quasi-planar parts of the nanotube wall are assumed to be formed by interstitial carbon atoms. The calculated equilibrium shape of collapsed nanotubes and the threshold diameter for permanently collapsed CNTs are found to agree with existing literature data. Elastic modulus, maximum stress, and strain at failure are calculated for zigzag CNTs with the equivalent diameter up to 6.27 nm in the temperature range from 5 K to 500 K. The simulations show that these mechanical properties only moderately depend on the diameter of circular CNTs. For collapsed CNTs with and without cross-links, the mechanical properties are practically independent of the CNT diameter for nanotubes with diameters larger than 4.7 nm. The elastic modulus and maximum stress of collapsed nanotubes are found to be smaller than those for the equivalent circular CNTs. The intra-tube cross-linking increases the elastic modulus and strength of collapsed CNTs in up to 50 % compared to corresponding collapsed CNTs without cross-links, but reduces the breaking strain. Thermal softening of CNTs with increasing temperature in the range from 100 K to 500 K induces a decrease in the elastic modulus and maximum stress in about 12-33 %.

## INTRODUCTION

Individual carbon nanotubes (CNTs) have excellent mechanical properties, e.g., [1-3]. The shear load transfer between pristine CNTs, however, is weak. As a result, CNT network materials like films, forests, and aerogels have low Young's modulus and strength. The load transfer between nanotubes can be improved by utilizing a few factors, including the increasing material density [4], twisting of CNT fibers, or covalent cross-linking of nanotubes [5-7]. In particular, in ultra-aligned CNT materials [8], the load transfer between CNTs is enhanced due to alignment of nanotubes and increased interfacial area. These materials usually consist of single- and double-walled CNTs of large diameters, which often exist in the collapsed form, e.g., in the form of nanotubes with "dog-bone"-shaped cross sections [9-12]. The presence of collapsed CNTs in super-aligned structures further improves the load transfer between nanotubes due to increased interfacial area and enhances mechanical properties of CNT materials [8,13].

The goal of this paper is to systematically study stretching properties of CNTs in a broad range of their diameters, which can exist in the form of nanotubes with circular cross sections, as well as in the form of "dog-bone"-shaped collapsed nanotubes with and without intra-tube covalent cross-links. As an additional factor, we also study the effect of thermal softening of CNTs at elevated temperatures. Although stretching of individual CNTs was a subject of numerous computational studies, e.g., [1-3,14-17], in the majority of these papers only CNTs of relatively small diameters with circular cross sections were considered. In the present paper, the simulations are focused on CNTs of larger diameters, including the nanotubes that can retain the collapsed shape at zero external pressure.

One of the interesting findings in our study is that the collapsed CNTs demonstrate much smaller variability in mechanical properties depending on the CNT chirality than their counterparts with circular cross sections. We also found that the intra-tube cross-linking can substantially increase the elastic modulus and strength of collapsed nanotubes with only


Copyright © 2018 by ASME

moderate reduction in the strain at failure. We plan to use the results obtained in the present paper for parametrization of recently developed mesoscopic model [17-19] designed for large-scale simulations of structural, mechanical, and thermal properties of CNT network materials.

## COMPUTATIONAL METHOD

Atomistic simulations are performed for three types of single-walled carbon nanotube (SWCNT) samples: CNTs with circular cross-sections (Figure 1(a)), collapsed CNTs with the cross sections of characteristic "dog-bone" shape (Figure 1(b)), and collapsed CNTs with covalent cross-links between parallel quasi-planar parts of the CNT wall (Figure 1(c)). We consider only collapsed CNTs of sufficiently large circumferences, which can retain the collapsed shape at zero external pressure and room temperature. The theoretical estimates of the minimum (critical) diameter of equivalent circular CNTs that can exist in the collapsed state at zero pressure are available from literature, e.g., [11,12].

An in-house computational code was developed in order to generate computational samples of single-walled straight and circular CNT of arbitrary chirality characterized by the chiral indices $(n,m)$ [20]. Non-equilibrium molecular dynamics (MD) simulations with generated SWCNT samples are performed with the LAMMPS simulation package [21]. The bonded and non-bonded van der Waals interaction between carbon atoms is described by the empirical AIREBO interatomic potential [22]. It is known that the original formulation of AIREBO strongly overestimates ductility of C-C bonds [23,24] and, correspondingly, the CNT breaking strain. In order to resolve this issue, we follow the recommendations in Ref. [23] and change the switching parameter of the AIREBO potential (parameter $r_{c,min}$ in the implementation of the AIREBO potential included into the LAMMPS package) from 1.7 Å to 1.95 Å. All MD simulations are performed with the time step of 0.1 fs.

In order to prepare a sample of a free-standing collapsed nanotube, we performed equilibrium MD simulations with a sample of initially circular nanotube in a triclinic computational cell with periodic boundary conditions in all three coordinate directions. The simulations are performed during 150 ps with the Nose- Hoover barostat at a pressure of 3 GPa and Nose-Hoover thermostat at a temperature of 5 K. In response to the applied pressure, the initially circular CNT gradually collapses and attains the shape with the "dog-bone" cross section shown in Figure 1(b). Then the applied pressure is released and the collapsed CNT is equilibrated during additional 100 ps without periodic boundary conditions in the directions perpendicular to the CNT axis at a temperature of 5 K.

In simulations, only cross-links formed by single interstitial carbon atoms are considered. The number of interstitial atoms is first calculated as $N_{CL} = n_{CL}L_T$, where $n_{CL}$ is the desired density of cross-links per unit nanotube length. Then individual interstitial atoms are added to the relaxed sample of a collapsed CNT one by one using the acceptance-and-rejection Monte Carlo method. For this purpose, we put the whole CNT into a rectangular computational box and generate random coordinates of a new interstitial atom. The new atom is added to the sample if (1) it is located within the cutoff distance of 2 Å of the bonded part of the AIREBO potential from at least two carbon atoms belonging to the opposite parallel parts of the CNT wall and (2) it is located farther than 2.5 Å from any other interstitial atom already added to the sample. Once the desired number of interstitial atoms is added to the CNT sample, the collapsed nanotube with interstitial atoms is equilibrated during 150 ps at a temperature of 5 K with periodic boundary conditions along the nanotube axis. After the relaxation, every CNT sample is inspected in order to ensure that all added interstitial atoms forms cross-links between neighboring parts of the CNT wall.

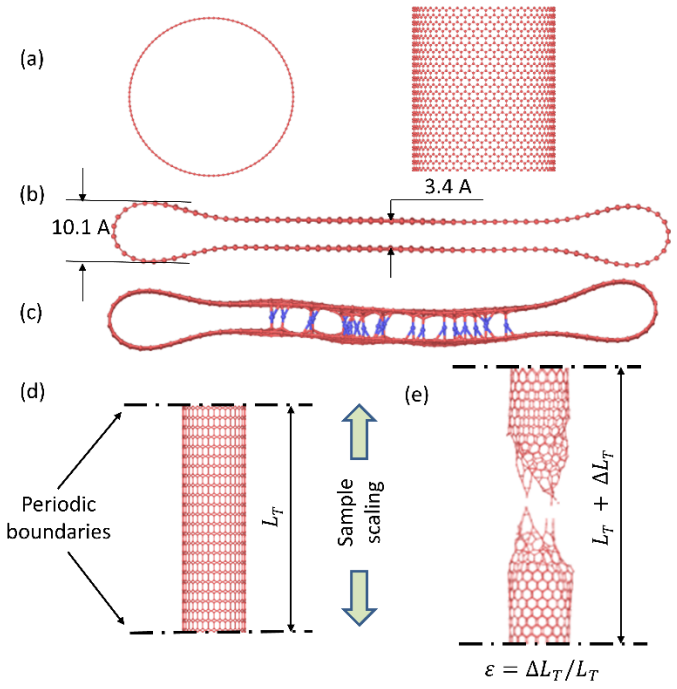


**Figure 1. Three types of single-walled CNT samples considered in simulations: CNT with circular cross section (a); collapsed CNT with a cross section of the "dog-bone" shape (b); and collapsed CNT with intra-tube cross-links formed by interstitial carbon atoms. In (c), bonds connecting interstitial atoms are shown in blue. Panel (d) illustrates the computational setup for quasi-static simulations of uniaxial stretching of CNTs: To implement stretching, the whole CNT sample is scaled along the CNT axis with the scaling velocity of 0.1 A per ps maintaining periodic boundary conditions in the direction along the axis of the nanotube. Panel (e) illustrates the typical shape of a broken CNT obtained with the modified AIREBO interatomic potential and switching parameter $r_{c,min} = 1.95$ Å.**


Copyright © 2018 by ASME

The relaxed CNT samples are subjected to the quasi-static stretching tests with periodic boundary conditions along the CNT axis. For this purpose, positions of atoms in whole CNT tube is scaled in the CNT axis with scaling velocity of 0.1 Å per ps, which induces permanent elongation of the nanotube (Figure 1(d)), maintaining periodic boundary conditions in the direction along the CNT axis. After every "scaling" time step, the whole system is relaxed during 10 ps using the Nose-Hoover thermostat algorithms at constant temperature $T$ and fixed sample length along CNT axis. This temperature was kept at a level of 5 K in all simulations shown in Figures 2-6 in order to study stretching properties of CNT in the limit of low temperatures. This limit is commonly considered in literature for |CNTs of relatively small diameters, e.g., Ref. [25]. Then the thermal softening of nanotubes is studied additionally, when the thermostat temperature $T$ varies from 100 K to 500 K (Figures 7-8). In every simulation, calculations are performed until fracture of the nanotube (Figure 1(e)).

In the course of mechanical loading, we calculate the total elongation of the nanotube $\Delta L_T$ (Figure 1(e)) and the instant total force $F$ exerted on atoms of the whole CNT from one side of the periodic cell. Then we calculate the engineering strain $\varepsilon = \Delta L_T / L_T$ and stress $\sigma = F/A_T$, where $A_T = \pi D_T \delta_T$ is the CNT cross-sectional area, $D_T$ is the CNT diameter (for collapse CNTs, $D_T$ is the diameter of a corresponding circular CNT), and $\delta_T = 3.4$ Å is the nominal thickness of the CNT wall taken to be equal to the interlayer spacing in graphite. The elastic modulus of CNTs is then determined as $E = \sigma_0/\varepsilon_0$, where $\sigma_0$ is the stress at strain $\varepsilon_0$, which is below the proportional limit. After a preliminary analysis of the stress-strain curves, a single value of $\varepsilon_0 = 0.005$ is chosen for calculations of the elastic modulus.

## RESULT AND DISCUSSION

We performed stretching simulations of a circular (10,10) SWCNT with both values of the parameter $r_{c,min}$, equal to 1.7 Å and 1.95 Å, in order to validate our computational setup and reveal the effects of calibration of the AIREBO potential by changing the parameter $r_{c,min}$. The obtained stress-strain curves are compared with results of atomistic simulations performed for SWCNTs of the same chirality based on the REBO empirical interatomic potential [26]. The simulations show that the increase of the parameter $r_{c,min}$ from to 1.7 Å to 1.95 Å practically does not affect the deformation of the nanotube in the elastic regime, but decreases the stress and the strain at failure. The elastic modulus of the CNT in our simulations is found to be equal to 1657 GPa. This value is in an agreement with a value of 1517 GPa, which we deduced from the stress-strain curve found in Ref. [27] for (10,10) CNTs based on the REBO potential (Figure 2). It is worth noting, however, that the elastic modulus $E = 1043$ GPa is reported for (10,10) CNTs in Ref. [27]. We found that this value can be calculated based on the stress-strain curve adopted from Ref. [27] assuming that $\varepsilon_0 = 0.042$. With this value of $\varepsilon_0$, our simulations result in $E = 1196$ GPa. Thus, for (10,10) CNTs, the values of the elastic modulus in our simulations agree with the values that can be deduced from results of Ref. [27] if the same $\varepsilon_0$ is used in both cases. These estimations also suggest that the sufficiently small value $\varepsilon_0 = 0.005$ is required for accurate calculations of $E$. At the same time, our simulations with the modified AIREBO potential predicts substantially smaller strain at failure compared to the results reported in Ref. [27]. All further results discussed in this Section and shown in Figures 3-8 are obtained with $r_{c,min} = 1.95$ Å.

The stress-strain curves obtained for circular zigzag nanotubes with the diameters ranging from 2.035 nm to 5.48 nm are shown in Figure 3. The simulations predict that the elastic modulus $E$ decreases with increasing CNT diameter from 1409 GPa at $D_T$ =2.035 nm to 1096 GPa at $D_T$ =5.48 nm (Figure 4). The variation of the strain at failure with the CNT diameter is non-monotonous (Figure 3), while the stress at failure $\sigma_{max}$ monotonously decreases with increasing $D_T$ (Figure 4). The variation of $E$ and $\sigma_{max}$ in Figure 4, however, is not large, and one can conclude that the simulations predict that the elastic and inelastic mechanical properties of CNT of large diameters only moderately depend on $D_T$.

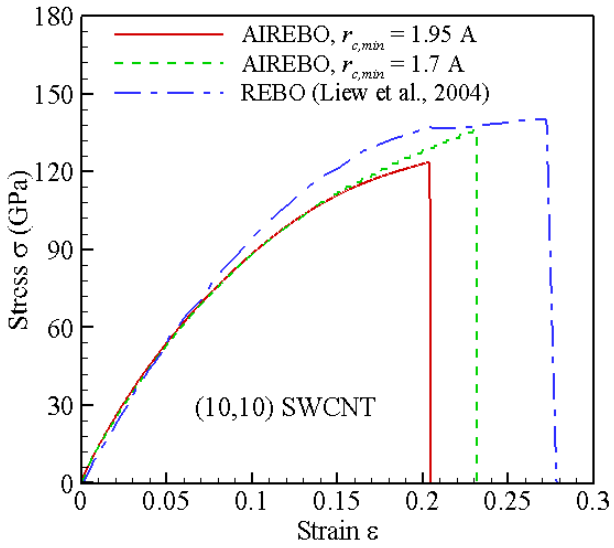


**Figure 2. Stress $\sigma$ versus strain $\varepsilon$ obtained in stretching simulations of a (10,10) SWCNT based on different interatomic potentials. Solid curve is obtained with the AIREBO potential at $r_{c,min} = 1.95$ Å. Dashed curve is obtained with the AIREBO potential at $r_{c,min} = 1.7$ Å. Dash-dotted curve is obtained with the REBO interatomic potential in Ref. [27].**

In simulations of collapsed nanotubes, we first define the critical diameter of zigzag nanotubes $D_c$ such that any nanotube with $D_T > D_c$ retains the collapsed shape after releasing the external pressure. The exact value of the critical diameter is known to be dependent on the interatomic potential adopted for simulations. For the modified AIREBO potential, our simulations show that $D_c$ is equal to 4.2 nm that corresponds to


Copyright © 2018 by ASME

(53,0) CNT. This value of the critical diameter is in the middle of the range of critical diameters from ~3 nm to ~6 nm reported in the literature for SWCNTs of various chirality [9-12]. After relaxation, the typical cross section of a collapsed SWCNT has a shape of a dog bone. The cross section of a nanotube obtained after collapsing (53,0) CNT is shown in Figure 1(b). The sizes of major geometrical features of the cross section of collapsed nanotubes, including the distance between parallel parts of the CNT wall and the size of the bulges, predicted in our simulations are in good agreement with the literature data [9-12].

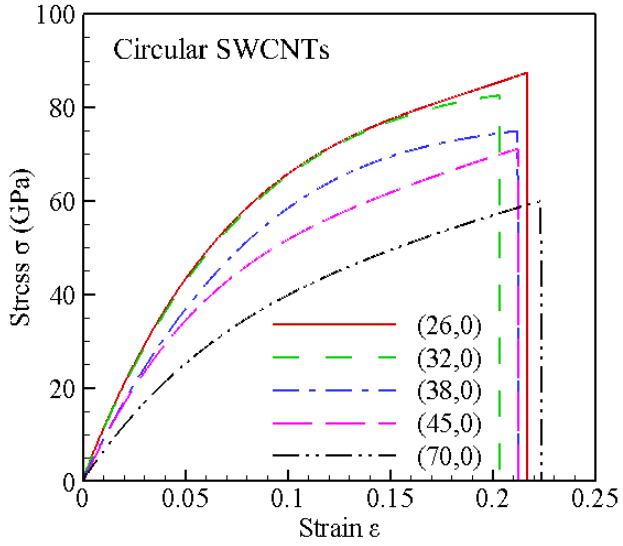


**Figure 3. Stress $\sigma$ versus strain $\varepsilon$ obtained in MD simulations of uniaxial stretching of circular zigzag SWCNT with various chirality and diameters ranging from 2.035 nm to 5.48 nm. The chirality indices corresponding to every curve are indicated in the figure panel.**

The stress-strain curves for a number of collapsed zigzag CNTs with $D_T > D_c$ are shown in Figure 5. The simulations reveal that collapsed CNTs have substantially smaller elastic modulus and stress at failure than their counterparts with circular cross sections. For instance, $\sigma_{max}$ for collapsed CNTs with dimeter larger than 4.7 nm is about 41 GPa, which is in 35-40% smaller than the stress at failure for corresponding circular CNTs (Figure 3), while the strain at failure for nanotubes of both types is practically the same and varies in the range from 0.2 to 0.24. It is interesting that the elastic and inelastic properties of collapsed nanotubes and their stress-strain curves become practically insensitive to size of the CNT, i.e., the diameter of the equivalent circular CNT, if $D_T$ is larger than 4.7 nm. This is the major distinct feature of the stretching behavior of collapsed nanotubes compared to circular CNTs, which have diameter-dependent properties in the whole considered range of $D_T$.

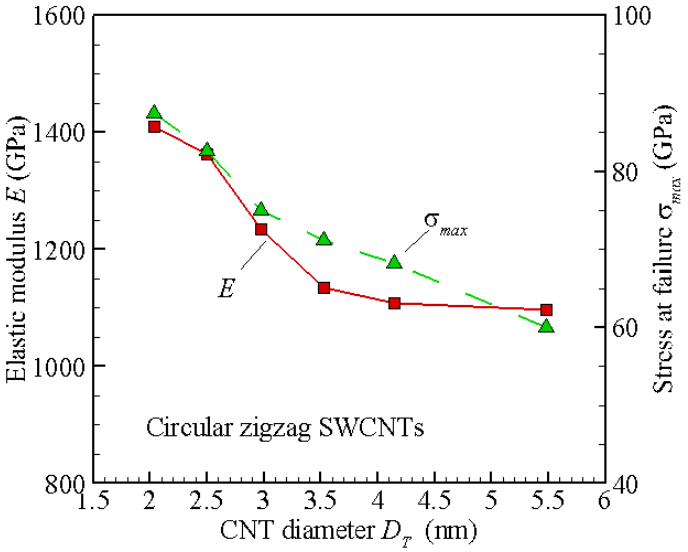


**Figure 4. Elastic modulus $E$ (squares) and stress at failure $\sigma_{max}$ (triangles) versus diameter $D_T$ of circular zigzag nanotubes. Symbols correspond to results of MD simulations, while curves are shown only to guide eye.**

For every CNT considered in Figure 5, we generate a corresponding collapsed nanotube with intra-tube cross-links connecting the opposing planar parts of the CNT wall at the linear cross-link density of 0.25 1/Å. According to the literature data [5,28], this value of cross-link density corresponds to a moderate density of atomic defects in the CNTs and is well below the amorphization threshold. The relaxed shapes of cross-linked CNTs are affected by the random distribution of cross-links and different from "ideal dog-bone" shapes of collapsed nanotubes without cross-links (Figure 1(c)). The stress-strain curves for collapsed CNTs with intra-tube cross-links are shown in Figure 6. The presence of cross-links increases the maximum stress in up to ~50%, but decrease the strain at failure in about 20%. In agreement with results of stretching simulations for collapsed CNTs without cross-links, the stress-strain curves for cross-linked CNTs are also independent of the equivalent CNT diameter if $D_T$ is large than 4.7 nm. The reduction in the breaking strain after cross-linking is expected, since the cross-linking introduces point defects in the crystal lattice of the CNT wall, making CNT more prone to fracture. The same effect is observed, e.g., during stretching of cross-linked CNT bundles [28]. An increase in the elastic modulus and strength after cross-linking, however, is a more intrigue feature. We plan to further investigate the mechanism of strengthening of collapsed CNTs via intra-tube cross-linking in our future work.


Copyright © 2018 by ASME

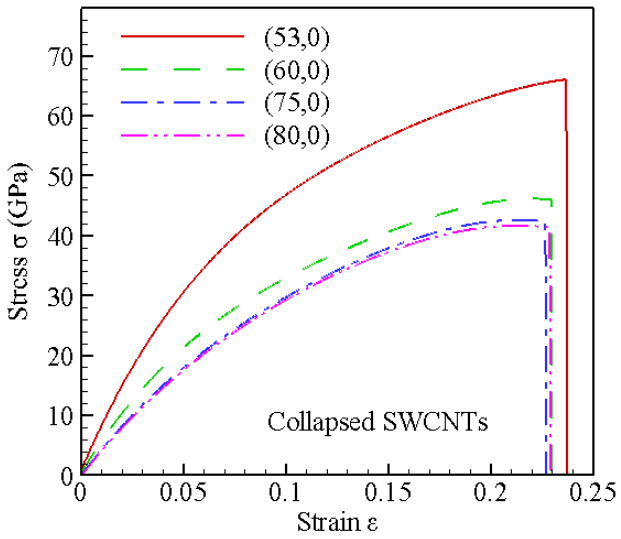


**Figure 5. Stress $\sigma$ versus strain $\varepsilon$ obtained in stretching simulations of collapsed zigzag SWCNT, obtained from circular CNTs with various chirality and diameters ranging from 4.2 nm to 6.27 nm. The chirality indices of the initial circular CNT corresponding to every curve are indicated in the figure panel.**

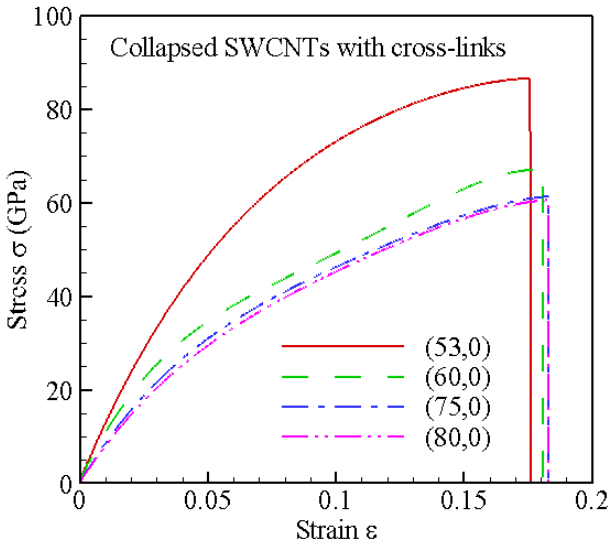


**Figure 6. Stress $\sigma$ versus strain $\varepsilon$ obtained in stretching simulations of collapsed zigzag SWCNT with covalent cross-links, obtained from circular CNTs with various chirality and diameters ranging from 4.2 nm to 6.27 nm. The linear density of cross-link is equal to $n_{CL} = 0.25$ 1/Å. The chirality indices of the initial circular CNT corresponding to every curve are indicated in the figure panel.**

In order to characterize the effect of temperature on the stretching properties of CNTs we perform stretching simulations of (53,0) circular CNT with temperature varying from 100 K to 500 K. The corresponding stress-strain curves are shown in Figure 7. An increasing temperature induces thermal softening of the CNT and reduces all major mechanical properties, including elastic modulus, strength, and strain at failure. In the considered temperature range, however, the overall changes in the mechanical properties are moderate and smaller than those that are induced by collapsing or covalent cross-linking of nanotubes. It is interesting that, at elevated temperatures, the linear regime of deformation, when the stress is proportional to the strain and the deformation behavior of a CNT can be expressed by Hook's law [17], occurs in a broader range of strain. For instance, at a temperature of 500 K, the stress is proportional to the strain up to a strain of 0.13, while already at 400 K the linear regime occurs only if the strain is smaller than 0.05.

The elastic modulus of the CNT decreases with increasing temperature from 829 GPa at $T = 100$ K to 628 GPa at $T = 500$ K, but tends to approach some asymptotic value of ~500 GPa at larger temperatures (squares in Figure 8). The dependence of $E$ on $T$ can be fitted by a quadratic polynomial shown in the panel of Figure 8. The strength of the CNT drops practically linearly from 75 GPa at $T = 100$ K to 60 GPa at $T = 500$ K (triangles in Figure 8). The dependence of $\sigma_{max}$ on $T$ can be fitted by a linear polynomial also presented in the panel of Figure 8. The coefficients of the both fitting polynomials are calculated based on the least square method.

## CONCLUSIONS

The systematic atomistic simulations are performed in order to investigate the effects of the CNT diameter, shape of the cross section, and intra-tube cross-linking by interstitial carbon atoms on the elastic and inelastic stretching properties of single-walled CNTs of large diameters. The simulations show that the nanotube diameter moderately affects the properties of CNTs with circular cross section, when both the elastic modulus and strength tend to decrease with increasing diameter. Collapsed nanotubes with and without cross-links demonstrate mechanical properties that are independent of the CNT diameter, if the dimeter is larger than 4.7 nm. The elastic modulus and strength of collapsed CNTs are found to be significantly smaller than those for CNTs with the circular cross section. Surprisingly, the intra-tube cross-links at moderate density significantly increase the elastic modulus and strength of collapsed nanotubes. Thermal softening of nanotubes at elevated temperature reduces the elastic modulus and strength, but increases the range of strain when stretching behavior of CNTs follows the linear relationship between stress and strain and, thus, can be described by Hook's law.

The obtained results can be used in order to parameterize the part of the mesoscopic forces field describing the stretching deformation of CNTs in the framework of the mesoscopic model developed in Refs. [17-19]. Once available, this parametrization will enable applications of the mesoscopic model for predicting structural, mechanical, and thermal


Copyright © 2018 by ASME

properties of network materials composed of CNTs of large diameters. We also plan to extend the computational approaches used in the present paper to simulations of load transfer in bundles of circular and collapsed multi-walled nanotubes with inter-wall and inter-tube cross-linking.

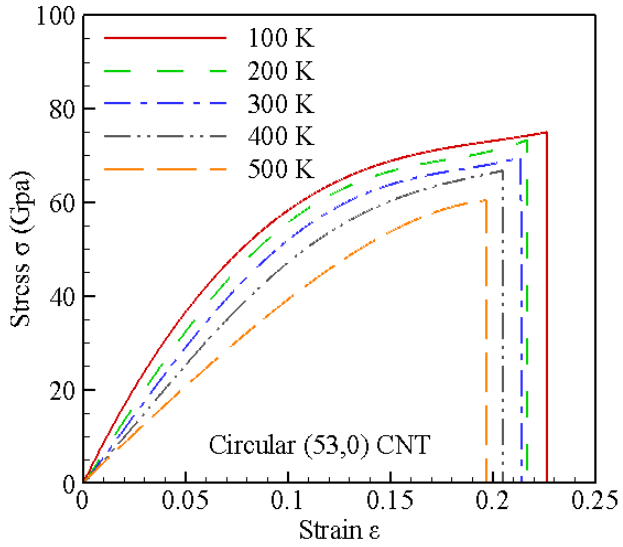


**Figure 7 Stress $\sigma$ versus strain $\varepsilon$ obtained in stretching simulations of circular (53,0) CNT at temperatures varying from 100 K to 500 K. Temperature for every curve is indicated in the figure panel.**

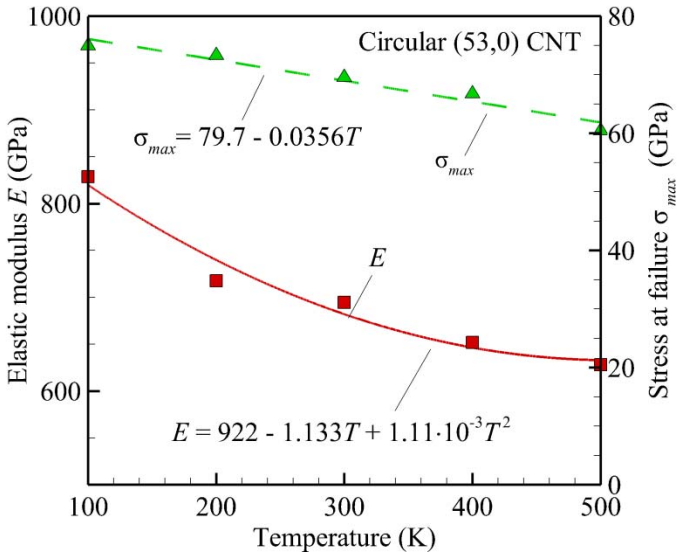


**Figure 8. Elastic modulus $E$ (squares) and stress at failure $\sigma_{max}$ (triangles) versus temperature obtained for circular (53,0) CNT. Symbols correspond to results of MD simulations. Curves correspond to the best polynomial fits of the calculated data. The fitting equations for $E$ and $\sigma_{max}$ are shown in the figure panel.**


## ACKNOWLEDGMENTS

This work is supported by the NSF through the CAREER award CMMI-1554589 and by NASA through Early Stage Innovations grant NNX16AD99G from NASA's Space Technology Research Grants Program. The computational support is provided by the Alabama Supercomputer Center. The authors thank Kaushik Joshi and Leonid Zhigilei for the help in modifying parameters of the AIREBO interatomic potential.


## REFERENCES


[1] Krishnan, A., Dujardin, E., Ebbesen, T.W., and Treacy, M.M.J., 1998, "Young's modulus of single-walled nanotubes," Phys. Rev. B **58**, pp. 14013–14019.

[2] Coluci, V.R., Pugno, N.M., Dantas, S.O., Galvao, D.S., and Jorio, A., 2007, "Atomistic simulations of mechanical properties of 'super' carbon nanotubes," Nanotechnology **18,** 335702.

[3] Bao, W.X., Zhu C.C., and Cui W.Z., 2004, "Simulation of Young's modulus of single-walled carbon nanotubes by molecular dynamics," Physica B. **352**, pp. 156-163.

[4] Zhang, G., Liu, C., and Fan, S., 2012 "High-density carbon nanotube buckypapers with superior transport and mechanical properties," Nano Lett. **12**, pp. 4848-4852.

[5] Kis,A., Csanyi, G., Salvetat, J.-P., Lee, T.-N., Couteau, E., Kulik, A.J., Benoit, W., Brugger, W., and Forro, L., 2004, "Reinforcement of single-walled carbon nanotube bundles by intertube bridging," Nat. Mater.. **3**, pp. 153-157.

[6] Pomoell, J.A.V., Krasheninnikov, A. V., Nordlund, K., and Keinonen, K., 2004, "Ion ranges and irradiation-induced defects in multiwalled carbon nanotubes," J. Appl. Phys. **96**, pp. 2864-2871.

[7] Salonen, E., Krasheninnikov, A.V., and Nordlund, K., 2002, "Ion-irradiation-induced defects in bundles of carbon nanotubes," Nucl. Instr. Meth. Phys. Res. B **193**, pp. 603-608.

[8] Zhang, X., Jiang, K., Feng, C., Liu, P., Zhang, L., Kong, J., Zhang, T., Li, Q., and Fan, S., 2006, "Spinning and processing continuous yarn from 4-inch wafer scale super-aligned carbon nanotube arrays," Adv. Mater. **18**, pp. 1505-1510.

[9] Elliott, J. A., Sandler, J. K.W., Windle, A. H., Young, R. J., and Shaffer, M. S. P., 2004, "Collapse of single-wall carbon nanotubes is diameter dependent," Phys. Rev. Lett. **92**, 095501.

[10] Tang, T., Jagota, A., Hui, C.-R., and Glassmaker, N.J., 2005, "Collapse of single-walled carbon nanotube," J. Appl. Phys. **97,** 074310.

[11] Félix, B., Le F.S., Adessi, C., Cerqueira T.F.T., Blanchard, N., Arenel, R., Brûlet, A., Marques, M.A.L.,



Copyright © 2018 by ASME

Botti, S., and San-Miguel, A., 2016, “Radial collapse of carbon nanotubes for conductivity optimized polymer composites,” Carbon **106**, pp. 64-73.

[12] Maoshuai, H., Jichen, D., Kaili, Z., Feng, D., Hua, J., Annick, L., Juha, L., and Esko, K.I., 2014, “Precise determination of the threshold diameter for a single-walled carbon nanotube to collapse,” ACS Nano, **8**, pp. 9657–9663.

[13] Motta, M., Moisala, A., Kinloch, I.A., and Windle, A.H., 2007, “High performance fibers from ‘dog bone’ carbon nanotubes,” Adv. Mater. **19**, pp. 3721-3726.

[14] Xian, S., and Xiaoqiao, H., 2017, “Hierarchical deformation of super carbon nanotube under tensile load,” ICMAE 17190723.

[15] Wong, E.W., Sheehan, P.E., and Lieber, C.M., 1997, “Nanobeam mechanics: elasticity, strength, and toughness of nanorods and nanotubes,” Science **277**, pp. 1971–1975.

[16] Talukdar, K., and Mitra, A.K., 2012, “A molecular dynamic simulation study for mechanical properties of different types of carbon nanotubes,” Appl. Nanoscience **2**, pp.377-383.

[17] Zhigilei, L. V., Wei, C., and Srivastava, D., 2005, “Mesoscopic model for dynamic simulations of carbon nanotubes,” Phys. Rev. B **71**, 165417.

[18] Volkov, A.N., and Zhigilei, L.V., 2010, “Mesoscopic interaction potential for carbon nanotubes of arbitrary length and orientation,” J. Phys. Chem. C **114**, pp. 5513-5531.

[19] Volkov, A.N., and Zhigilei, L.V., 2010, “Structural stability of carbon nanotube films: The role of bending buckling,” ACS Nano **4**, pp. 6187-6195.

[20] Jishi, R.A., Venktaraman, L., Dresseshaus, M.S., and Dresselhaus, G., 1995 “Symmetry properties of chiral carbon nanotube,” Phys. Rev. B **51**, pp. 11176-11179.

[21] Plimpton, S., 1995, “Fast parallel algorithms for short-range molecular dynamics.” J. Comp. Phys. **117**, pp. 1–19.

[22] Stuart, S.J., Tutein, A.B., and Harrison, J.A., 2000, “A reactive potential for hydrocarbons with intermolecular interactions,” J. Chem. Phys. **112,** pp. 6472-6486.

[23] Zhan, H., Zhang, G., Tan, V. BC, Cheng, Yuan, Bell, J. M. Zhang, Y.-W., and Gu, Y., 2016, “From brittle to ductile: A structure dependent ductility of diamond nano thread,” Nanoscale **8**, pp. 11177-11184.

[24] Xueming, Y., Sihan, W., Jiangxin, X., Bingyang, C., and Albert, T.C., 2018, “Spurious heat conduction behavior of finite-size graphene nanoribbon under extreme uniaxial strain caused by the AIREBO potential,” Nanotechnology **17**, pp. 1323-1332.

[25] Lu, Q., and Bhattacharya, B., 2006, “Fracture resistance of zigzag single walled carbon nanotubes,” Physica E **96**, pp. 46-53.

[26] Brenner, D. W., Shenderova, O. A., Harrison, J. A., Stuart, S. J., Ni, B., and Sinnott, S. B., 2002, “A second-generation reactive empirical bond order (REBO) potential energy expression for hydrocarbons,” J. Phys.: Condens. Matter **14**, pp. 783–802.

[27] Liew, K.M., He, X.Q., and Wong, C.H., 2004, “On the study of elastic and plastic properties of multi-walled carbon nanotubes under axial tension using molecular dynamics simulation,” Acta Materialia **52**, pp. 2521-2527.

[28] O’Brien, N. P., McCarthy, M. A., and Curtin, W. A., 2013, “A theoretical quantification of the possible improvement in the mechanical properties of carbon nanotube bundles by carbon ion irradiation,” Carbon **53**, pp. 346-356.


Copyright © 2018 by ASME